Asikainen, Sanja; Paakinaho, Kaarlo; Kyhkynen, Anna Kaisa; Hannula, Markus; Malin, Minna; Ahola, Niina; Kellomäki, Minna; Seppälä, Jukka

Hydrolysis and drug release from poly(ethylene glycol)-modified lactone polymers with open porosity

Published in:
European Polymer Journal

DOI:
10.1016/j.eurpolymj.2019.01.056

Published: 01/04/2019

Document Version
Peer-reviewed accepted author manuscript, also known as Final accepted manuscript or Post-print

Hydrolysis and Drug Release from Poly(Ethylene Glycol)-Modified Lactone Polymers with Open Porosity

Sanja Asikainen[1], Kaarlo Paakinaho[2,3], Anna-Kaisa Kyhkynen[4], Markus Hannula[5], Minna Malin[1], Niina Ahola[4], Minna Kellomäki[4,6] and Jukka Seppälä[1*]

1 Polymer Technology Research Group, School of Chemical Engineering, Aalto University, Finland

2 Adult Stem Cell Group, BioMediTech, Faculty of Medicine and Life Sciences, University of Tampere, Tampere, Finland

3 Orton Orthopaedic Hospital, Helsinki, Finland

4 Biomaterials and Tissue Engineering Group, BioMediTech, Faculty of Biomedical Sciences and Engineering, Tampere University of Technology, Finland

5 Computational Biophysics and Imaging Group, BioMediTech, Faculty of Biomedical Sciences and Engineering, Tampere University of Technology, Tampere, Finland

6 BioMediTech, Faculty of Medicine and Life Sciences, University of Tampere, Tampere, Finland

*corresponding author, e-mail: jukka.seppala@aalto.fi

ABSTRACT

The ability to release active agents from a porous scaffold structure *in situ* enables the simultaneous structural support for the cells proliferating and differentiating towards tissue as well as the stimulation of tissue regeneration. Due to the great potentiality of such approach, drug-releasing scaffolds were fabricated from hydrolytically degradable polymers. Three copolymers of poly(ethylene glycol), ε-caprolactone, L- and D,L- lactide were synthesized and blended with bone-growth inducing active agents, dexamethasone (DM) and 2-phospho-L-ascorbic acid trisodium salt (AS). Porous scaffolds were prepared by means of super-critical carbon dioxide foaming.

In the final scaffold structures, the particle size, location and the water solubility of the drug affected the release kinetics. As the large and water soluble AS particles were more exposed to the buffer solution compared to small DM particles, the AS release was burst-like whereas DM showed a long-term release. The material structure had a significant effect on the release kinetics as the porous scaffolds released active agents faster compared to the solid cylinders. Furthermore, this study showed the strong effect of polymer degradation and wettability on the release, which were more determinative than the pore architecture.

Keywords: drug release, supercritical carbon dioxide foaming, hydrolytic degradation, dexamethasone, 2-phospho-L-ascorbic acid trisodium salt, bulk degradation

1. INTRODUCTION

Bone is the second most common transplantation tissue in human body [1,2], with over 2 million bone graft procedures being performed annually [3]. The golden standard for bone substitution is autograft, where the bone graft is harvested from the patient [2,3]. The autograft is usually considered the ideal bone graft material, however donor site complications are possible and bone availability in pediatric and elderly patients is limited [2,4,5]. Therefore, the clinical need for synthetic bone grafts is increasing due to an aging population [5].

Non-autologous, synthetic bone graft products commercially available are mainly ceramic based materials, which are widely used in clinical practice [2,6]. Composites of ceramics and resorbable polymers have been researched with the aim to produce bioactive tissue engineering scaffolds. Scaffold bioactivity has been attempted to achieve with osteconductive and osteoinductive agents, such as growth factors [7], hydroxyapatite (HA) [8,9], tricalcium phosphate (TCP) [10,11] and bioactive glass (BAG) [12]. The bone-growth inducing active agents used in osteogenic differentiation media, β-glycerophosphate, dexamethasone and ascorbic acid [13–15], have not been as widely incorporated into polymer scaffolds, even though they have been extensively used in cell cultivation. The function of β-glycerophosphate is to provide phosphate ions for mineralization [14]. Dexamethasone (DM) has been shown to induce proliferation, maturation and mineralization of osteoblasts *in vitro* and *in vivo* [14–18] and it also inhibits inflammatory processes [19]. Ascorbic acid stimulates collagen synthesis [20] and has been used in osteogenic cell differentiation with dexamethasone and β-glyserophosphate [13]. However, ascorbic acid is an unstable compound and therefore more stable derivatives are often used [21].

In the early phase of development of resorbable polymers, research was focused on two-dimensional structures, such as fixation devices and plates, and therefore several commercially available solutions are on the market [6]. Nowadays, the focus is on three-dimensional porous structures, which enable tissue to regenerate and grow throughout the resorbing scaffold. Ideally, the regenerative bone tissue engineering scaffolds should be highly porous [22] and the pores should be interconnected to enable cell in-growth [2,5,23]. There are conflicting reports on the optimal pore size for bone tissue engineering [24]. Many studies show that the pore size should be in the range of 100-500µm for bone cells [2,5,22,24], however, smaller and larger pore size (20-1500µm) have also been used in bone tissue engineering [24]. Porous structures can be prepared with various techniques, such as using porogen agents, additive manufacturing (AM) and supercritical carbon dioxide ($scCO_2$) foaming.

$scCO_2$ foaming is an environmentally friendly and inexpensive way to produce porous structures, even in industrial large-scale manufacturing. The process is operated at low temperature without organic solvents, which may allow the use of thermosensitive molecules/compounds and even cells [25]. It has been shown that the foaming process may remove unreacted monomers, catalysts and initiators from the polymer [26] and it has also been used for sterilization under specific conditions [27]. During the foaming process, high pressure CO_2 plasticizes the polymer and pores are formed as the CO_2 escapes from the polymer. The processing parameters (CO_2 saturation pressure, soaking time, temperature, and depressurization rate) can be adjusted to control the pore architecture [25,28] making $scCO_2$ foaming an extremely promising option for the preparation of interconnected and highly porous structures. $scCO_2$ processing results in the formation of a polymer skin on the sample [27,29] that is, however, easy to remove with a sharp blade or machining.

CO_2 solubility and diffusivity are greatly influenced by the molecular structure of the polymer. Dissolution of CO_2 is enhanced if there are carbonyl or ether groups in the polymer, since it is based on Lewis acid-base interactions, where CO_2 has Lewis acidity in the carbon atom, and the polymer contains Lewis base sites. [30] Therefore, poly(ethylene glycol) (PEG) has stronger interactions with CO_2 compared to polyesters. Polymer crystallinity also affects the foaming process since CO_2 has relatively low solubility and slower diffusivity in highly crystalline polymers, since crystallinity reduces the amount of accessible free volume. [27,30,31]

Several neat polymers have been porogenized with $scCO_2$ for biomedical applications: poly(caprolactone-co-lactide) [10], poly(L-lactide) [31], poly(D,L-lactide) [28,31], poly(pentadecalactone-co-caprolactone) [32], and poly(methyl methacrylate) [33]. In addition, composites of poly(caprolactone-co-lactide) and TCP has been used successfully foamed [34]. Some polymer and drug or growth-factor combinations have been studied, such as, polycaprolactone (PCL) [35,36], poly(D,L-lactide-co-glycolide) (PLGA) [7], poly(D,L-lactide) [37,38] and poly(methyl methacrylate)–poly(l-lactic acid) (PMMA–PLA) blends [39].

In this study, three PEG-P(CL-co-LA) polymers with different monomer ratios were synthetized and blended with bone-growth inducing agents dexamethasone (DM) and ascorbic acid derivative 2-phospho-L-ascorbic acid trisodium salt (AS). The polymers were porogenized with $scCO_2$ and drug release from the porogenized and solid samples were monitored for 20 weeks. It can be hypothesized that incorporating poly(ethylene glycol) into the back-bone of P(CL-co-LA) would increase the hydrophilicity of the polymer. Increased hydrophilicity would improve the wettability of porous samples, which is beneficial as some of the pores formed by $scCO_2$ are small. To the best of the authors' knowledge, there have

been no previous studies regarding $scCO_2$ foamed PEG-P(CL-co-LA) scaffolds releasing bone-growth inducing active agents.

2. MATERIALS AND METHODS

2.1. Materials

Prior to the polymerization of experimental polymers, ε-caprolactone (Fluka) was distilled and L- and D,L- lactide (Corbion) were dried in vacuum. Sn(II)octoate (stannous 2-ethylhexanoate) (Sigma-Aldrich) was the initiator and used as received. Linear poly(ethylene glycol) with OH-end groups (PEG, average M_n 20 000g/mol) (Sigma-Aldrich) was used as a co-initiator and dried in vacuum prior use. Medical grade poly(L-lactide-co-ε-caprolactone) 70/30 from Corbion (code PLC 7015) was used as a reference polymer.

Active agents, 2-phospho-L-ascorbic acid trisodium salt (AS, 95%, Sigma-Aldrich) and dexamethasone (DM, 98%, Sigma-Aldrich), were used as received. The water solubility of AS and DM are 32g/1000g and 0.09g/1000g, and molecular weight 322.05g/mol and 392.46g/mol, respectively. Potassium dihydrogen phosphate (KH_2PO_4) (J.T. Baker) and sodium phosphate dibasic anhydrous (Na_2HPO_4) (J.T. Baker) were used to prepare Sörensen buffer solution according to ISO 15814 standard (Implants for surgery – Copolymers and blends based on polylactide – In vitro degradation testing).

2.2. Polymer synthesis and characterization

Polymer synthesis was carried out in bulk under nitrogen atmosphere in a conically shaped batch reactor (Design Integrated Technology Inc., 4CV Helicone Mixer) at 160 °C. The amount of co-initiator PEG was 0.04mol-% and initiator Sn(II)octoate 0.05mol-% respective to the amount of monomers. Polymerization times were 3h15min for PEG-P(CL30-LLA70), 4h30min

PEG-P(CL30-DLLA70) and 4h20min for PEG-P(CL15-DLLA85). Polymers were dissolved into dichloromethane (99.8%, Merck KGaA) and precipitated from ethanol (Etax B, Altia Oyj). Polymers were stored in vacuum before further use to prevent moisture in air from degrading the polymers. The compositions of synthetized polymers were confirmed by ^{13}C NMR (Bruker Ultrashield 400Hz) [40]. Peaks for CL-units were observed at 172 and 173 ppm, LA-units at 170 and 169 ppm and PEG-unit at 70 ppm (Fig. S1). Figure 1 presents the skeletal formula of the polymers and Table 1 the abbreviations of polymers used in this study. P(CL30-LLA70) was commercial reference.

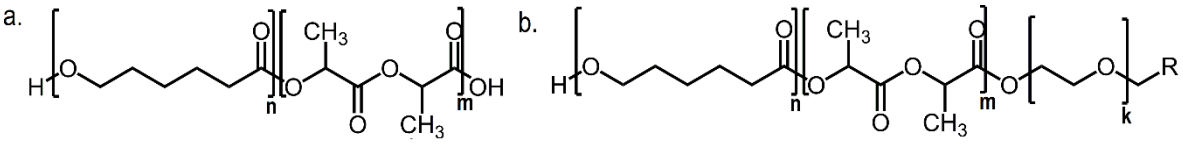

Figure 1. Skeletal formula of a. P(CL-LA) and b. PEG-P(CL-LA).

Table 1. Abbreviations of copolymers, co-monomer amounts and lactide type in feed.

Copolymer	CL-content (mol -%)	LA-content (mol -%)	Lactide type	PEG as co-initiator
P(CL30-LLA70)	30	70	L	N/A
PEG-P(CL30-LLA70)	30	70	L	Yes
PEG-P(CL30-DLLA70)	30	70	DL	Yes
PEG-P(CL15-DLLA85)	15	85	DL	Yes

Capillary viscometry was used for analyzing inherent viscosities (IV). Measurements were performed using a Lauda capillary viscometer (Lauda-Königshofen) with Ubbelohde capillaries (Schott-Instrument) and chloroform (99.0-99.4%, Merck KGaA) as a solvent at 25 °C. Two parallel polymer samples were measured with a concentration of 1mg/ml. Sufficiently-high IV (≥1 dl/g) was required for reproducible foaming process with the equipment used in this study.

Thermogravimetric analysis (TGA 500, TA Instruments) was used to study the decomposition temperatures of the polymers. Analysis was conducted by heating the polymer samples (19±2mg) at rate of 20°C/min up to 600°C under synthetic air.

2.3. Blending of active agents

Polymer and active agent (4 and 8wt-%) was fed into a twin screw midi-extruder (DSM, capacity of 16 cm3 with screw length 150mm) under nitrogen atmosphere. The blend was fed and mixed once (10min, 65rpm), extruded and fed again and mixed for an extra 2 minutes. Extrusion temperatures for P(CL30/LLA70), PEG-P(CL30-LLA70), PEG-P(CL30-DLLA70) and PEG-P(CL15-DLLA85) were 145°C, 140°C, 125°C and 100°C, respectively. The temperatures used were chosen based on the rheological properties of polymers. Used temperatures were as low as possible to avoid destroying the active agents. Neat polymers were also extruded to obtain similar processing history for the samples. After extrusion, materials were compression molded (Fortune TB 400) with 150kN pressure using the same processing temperatures to form cylinders with diameter 5mm and height 2 mm for hydrolysis and drug release. These compression-molded samples were used also in $scCO_2$-foaming.

Thermogravimetric analysis (TGA) showed polymer decomposition above 250°C. Differential scanning calorimetry (DSC) was used to evaluate the homogeneity of the blends and to measure glass transition temperatures (T_g) and melting temperatures (T_m) of extruded and heat pressed samples (5-10mg). DSC analysis was performed with a DSC Q1000 and Q2000 (TA Instruments, Delaware, USA) under nitrogen atmosphere. For the Q1000, two heating scans were performed (20°C/min) from -20°C to 200°C with 1 minute isothermal section at 200°C and cooling at rate of -50°C/min. T_g was analyzed from the second heating and T_m from the first. The first DSC runs were conducted until 200°C, because according to TGA, the

decomposition of polymers begins when the temperature increases above 250 °C. According to material safety data sheets, DM has a melting point at 262-264°C and AS at 260°C. Therefore, to study the homogeneity of the blends, heating scans with a rate of 10°C/min from -20°C to 300°C were conducted later with the DSC Q2000. For the analysis of the results, TA Universal analysis software was used.

2.4. Foaming and micro-CT analysis

Porous samples were obtained using supercritical carbon dioxide ($scCO_2$) foaming. Compression molded polymer cylinders (diameter 5mm, height 2 mm) were used in the foaming. Processing was conducted using high pressure and 90°C temperature in presence of CO_2. The foaming process utilized the same settings for all polymers. Prior to active agent release and hydrolysis studies, polymer skin was manually removed with a sharp knife.

Micro-CT imaging was performed in order to achieve information about the scaffolds' 3D geometry and active agent particles in scaffolds. Scaffolds were stacked on top of each other and 1600 x-ray projections from 360° were acquired with a Xradia MicroXCT-400 x-ray imaging system (Carl Zeiss X-ray Microscopy Inc.). Source voltage was 80 kV and source current 125 µA. A 4x objective was used with 2 binning which resulted 6.2 µm voxel size. Projections were reconstructed with XMReconstructor provided by the device manufacturer. After reconstruction, image thresholds were adjusted manually. Porosities and pore sizes were calculated from micro-CT images with Fiji [41] using the BoneJ [42] plugin. In this study, open porosity was outlined to the proportion of the internal pore space accessible by a sphere of 12µm diameter. All visualizations were conducted with Avizo 9.3.0 Software (Thermo Fisher Scientific, Waltham). Active agent powder particle sizes were evaluated using scanning electron microscope (SEM, TM-1000, Hitachi).

2.5. Contact angle measurements

Contact angle measurements were performed by depositing a 7μl size droplet of distilled water through a syringe onto the surface of polymer film (KSV Contact angle measurement system and software). Samples were prepared by melting polymer in an oven between two metal plates and polyethylene terephthalate sheets for 20 minutes at 180°C. Subsequently, polymer films were cooled at room temperature between two metal plates. Dry samples were stored in vacuum for two weeks before contact angle measurements. In order to measure the effect of buffer solution on the contact angle, polymer films were immersed in phosphate buffer solution pH 7.4 (FF-Chemicals Oy) for 24 hours before measurement and their surface was dried quickly with compressed air prior to measurement.

2.6. Mass loss and degradation

Mass loss and degradation behavior of polymers were studied according to ISO 15814 standard by immersing the solid and porous cylindrically shaped polymer samples (diameter 5mm, height 2mm, n=3) in 10ml of Sörensen buffer solution (pH 7.4), which was replaced with fresh solution in every two weeks. Samples were mildly agitated at 100rpm at 37°C. Samples were dried in vacuum for at least 1 week and weighed. Polymer swelling was studied by immersing the solid samples in Sörensen buffer solution and weighing the surface dried samples immediately after immersion and again after drying in vacuum.

For degradation studies, polymers from the mass loss study were dissolved in chloroform at a concentration of 10ppm. Dispersity was determined using size exclusion chromatography utilizing a Waters Associates system equipped with a Waters 717Plus Satellite autosampler, a Waters 510 HPLC solvent pump, four linear PL gel columns (104, 105, 103, and 100 Å) connected in series, and a Waters 2414 differential refractometer. The number average

molecular weight (M_n) and weight-average molecular weight (M_w) of the samples were determined against polystyrene standards at room temperature.

2.7. Active agent release and stability

Unicam UV 500 UV-Vis-Spectrophotometer (Thermo Spectronic, Cambridge, England) was used to analyze the active agent release by using calibration curves and to evaluate the stability of the active agents in Sörensen buffer solution. Stability was tested by dissolving active agents (40µg/ml) in Sörensen buffer solution and monitoring the concentration for one week. Active agent release and stability studies were conducted in the same conditions as swelling and hydrolysis studies.

3. RESULTS

3.1. Molecular weights and inherent viscosity

Molecular weights, dispersity (D) and inherent viscosity of the polymer samples are presented in Table 2. As shown, $scCO_2$ processing decreased the molecular weights of the PEG-containing polymers. In addition, blending with AS decreased the molecular weights 15% on average, whereas DM did not have an effect on the molecular weights. Inherent viscosity of P(CL30-LLA70) was also affected by the processing (extrusion and heat press) showing a decrease in the IV value from 1.5 to 1.0dl/g.

Table 2. Measured M_w and M_n for porous and nonporous polymer samples (n=2). Inherent viscosity (IV) of heat pressed polymer samples, prior to $scCO_2$ processing (n=2).

	Solid samples (g/mol)			Porous samples (g/mol)			IV
Polymer	M_w	M_n	D	M_w	M_n	D	(dl/g)
P(CL30-LLA70)	235000	142000	1.7	232000	140000	1.7	1.0
PEG-P(CL30-LLA70)	78000	50000	1.6	65000	45000	1.4	0.8
PEG-P(CL30- DLLA70)	152000	88000	1.7	138000	92000	1.5	1.3
PEG-P(CL15- DLLA85)	220000	147000	1.5	157000	97000	1.6	1.6

3.2. Thermal analysis and active agent solubility on polymer

DSC analysis showed neat, L-lactide containing polymers displaying crystallinity. P(CL30-LLA70) had a melting peak with low enthalpy which was also visible in the first heating cycle of the heat pressed sample. However, P(CL30-LLA70) samples containing active agents did not show crystallinity. PEG-P(CL30-LLA70) on the other hand was also semi-crystalline as a blend.

According to the material safety data sheets, DM has a melting peak at 262-264°C and AS at 260°C. In the DSC scans, DM had a melting peak at 262°C and blends had melting peaks in the range 200-212°C. The melting peak for AS at 260°C is not visible in DSC graph. Instead, neat AS has an exothermic peak at 228°C and the comparable peak in polymer blends varied from 210 to 223°C. Results of DSC scans are shown in Table 3.

Table 3. DCS results of DM, AS, PEG, polymers and polymer blends after processing. The theoretical amounts of AS and DM in the polymer blends are 8 wt-%.

Sample	Tg (ºC)	Tm (ºC) polymer	Enthalpy (J/g)	Tm (ºC) AS/DM
DM	-	-		262
AS	-	-		228
PEG 20000	-	64		N/A
P(CL30-LLA70)	23	108	4.6	N/A
P(CL30-LLA70) AS	23	-		219
P(CL30-LLA70) DM	24	-		212
PEG-P(CL30-LLA70)	20	145	23.6	N/A
PEG-P(CL30-LLA70) AS	18	145	25.4	210
PEG-P(CL30-LLA70) DM	21	144	22.4	204
PEG-P(CL30-DLLA70)	35			N/A
PEG-P(CL30-DLLA70) AS	35			223
PEG-P(CL30-DLLA70) DM	37			204
PEG-P(CL15-DLLA85)	29			N/A
PEG-P(CL15-DLLA85) AS	31			216
PEG-P(CL15-DLLA85) DM	31			200

TGA analysis showed degradation of polymers above 250°C and DM above 230°C. 2.5% of AS decomposed already in the range of 90 to 200°C. The low decomposition temperature of AS most probably affected the decrease of molecular weight of AS-containing polymers during processing.

In addition to DSC, the blending of active agents with the polymer and amounts of particles in blends can be evaluated using micro-CT (Figure 2). The active agent particles have been detected from an area of 3x3x1mm. Particles smaller than 7.6µm are not included in the micro-CT analysis due to the resolution and accuracy of the analysis method. The active agent powders contain smaller than 7µm particles as evaluated by SEM (Fig S2).Therefore, the samples may contain also smaller particles than 7.6µm or active agents that are dissolved in the polymer. Qualitatively, DM containing samples have significantly less detected particles in micro-CT analysis and the particles are smaller compared to particles of AS blends. The diameter of an AS particle on average is 18µm and DM particle 11µm. Almost all of the DM particles are smaller than 50µm in diameter. On average, DM samples have only a few particles larger than 40µm in diameter, whereas those of AS have hundreds of particles. In all of the samples, most of the particles have diameters in the range of 7 to 20µm.

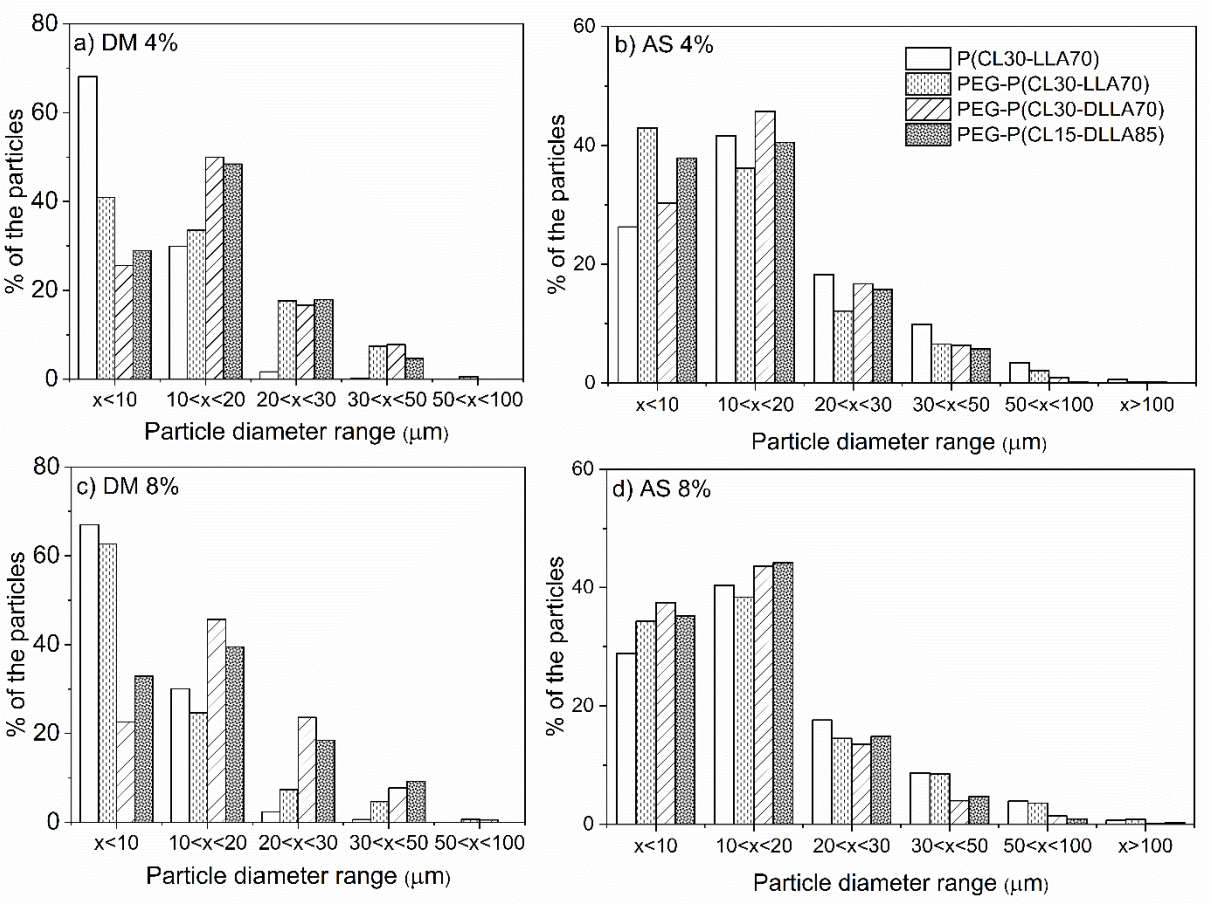

Figure 2. Particle diameter range in blends analyzed with micro-CT. Blends contained a) 4wt-% of DM, b) 4wt-% of AS, c) 8wt-% of DM and d) 8wt-% of AS.

Even though the number of these small particles is significant, their volume fraction is small as can be seen in the Table 4. Reference polymer P(CL30-LLA70) with dexamethasone is an exception having larger volume fractions of small particles in both of the blends (dexamethasone content of 4% and 8%). Since all blends were prepared similarly, it might be that P(CL30-LLA70) and DM are chemically more compatible with each other and thus part of the DM is dissolved in the polymer.

Table 4. Volume fractions of small (<20μm) and large (>20μm) particles in different blends. Particle diameter 20μm corresponds to volume 4189μm^3.

	AS 4%		AS 8%		DM 4%		DM 8%	
	large	small	large	small	large	small	large	small
P(CL30-LLA70)	96	4	96	4	21	79	34	66
PEG-P(CL30-LLA70)	91	9	97	3	82	18	79	21
PEG-P(CL30-DLLA70)	85	15	86	14	76	24	81	19
PEG-P(CL15-DLLA85)	78	22	88	12	75	25	80	20

3.3. Pore structure

Pore architectures of the foamed samples were studied with micro-CT. Analysis focused on determining porosity, amount of open pores, average pore size, wall thickness, surface area to volume ratio (Table 5) and pore size range (Figure 3). Semi-crystalline PEG-P(CL30-LLA70) displayed the lowest porosity range of 19-31%, whereas other samples exhibited porosities in the range of 57-72%. The majority of the pores (>99.9%) were open to the surface, except PEG-P(CL30-LLA70) having open porosity in the range of 83-95%. Semi-crystalline PEG-P(CL30-LLA70) had the smallest pore size range of 31-58μm.

Figure 3 shows pore size range of different polymer samples containing 8wt-% of DM. Other polymer and active agent combinations follow the same trend: most of the pores in PEG-P(CL30-LLA70) are small and there are only a few larger pores, whereas other polymers have broader pore size range.

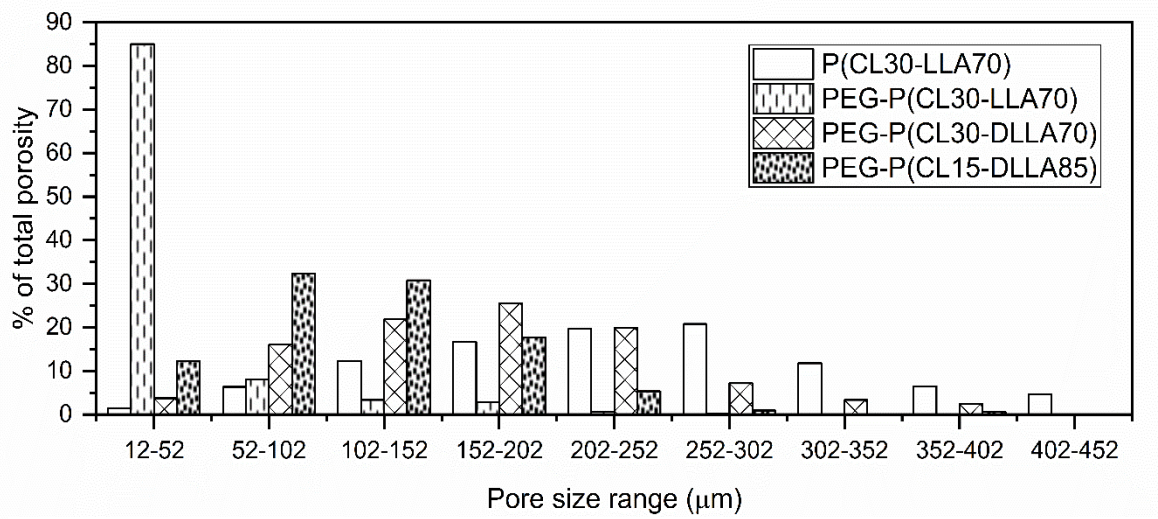

Figure 3. Pore size range of polymer samples containing 8wt-% dexamethasone.

Table 5. Porosity, pore size, wall thickness and area/volume of porous polymer blend samples containing 4% and 8% of AS and DM.

Sample	Porosity (%)
P(CL30-LLA70) AS 4	62
P(CL30-LLA70) AS 8	60

Wall thickness correlates with pore size; polymers with large pores generally have a larger wall thickness. PEG-P(CL15-DLLA85) has, however, a smaller wall thickness and average pore

size compared to other polymers. Figure 4 presents porous structures with micro-CT images, where large AS particles are can be detected as white spots.

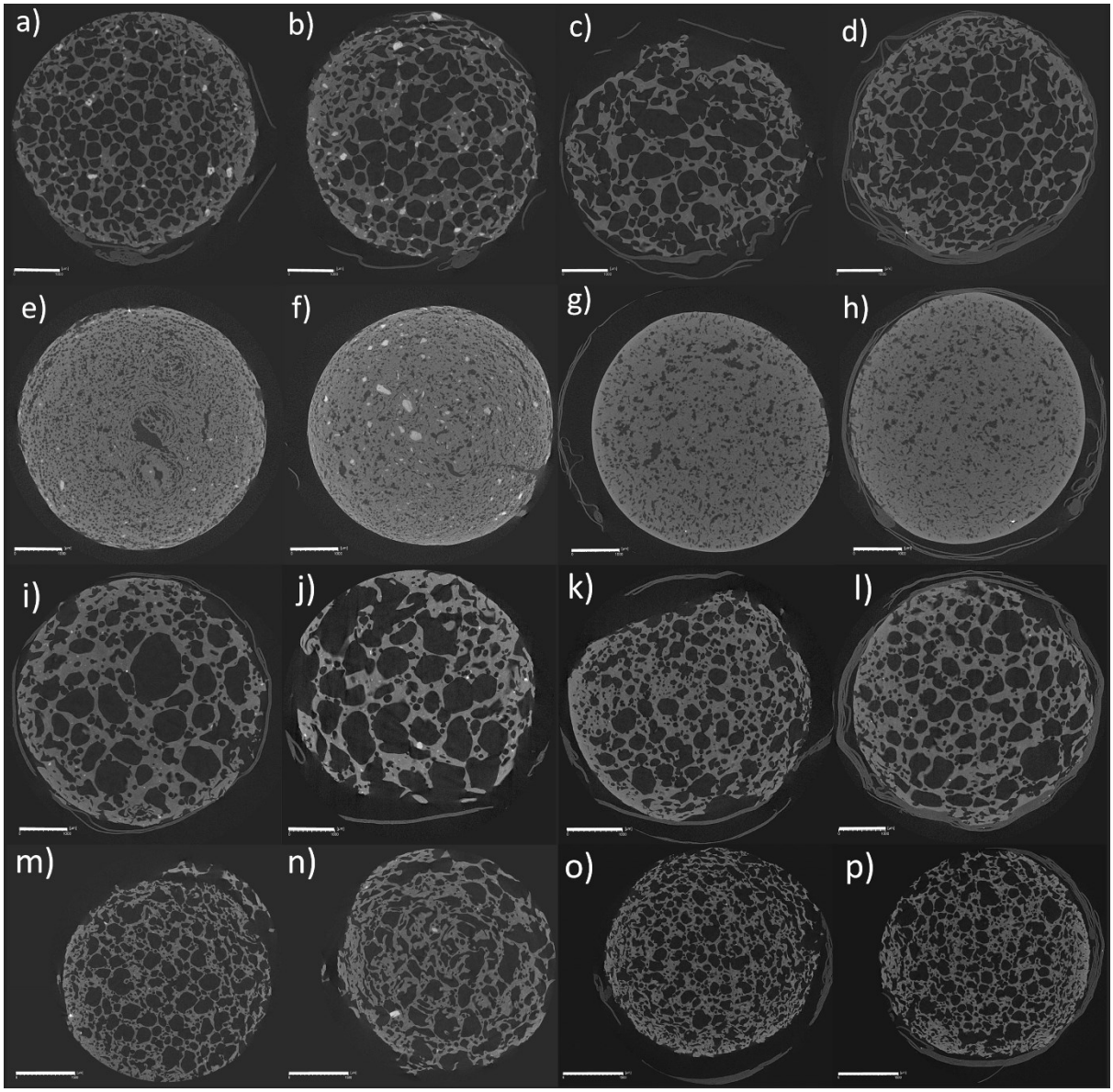

Figure 4. 2D µCT-images of porous samples containing ascorbic acid salt (AS) and dexamethasone (DM). P(CL30-LLA70) a) 4 wt-% AS, b) 8 wt-% AS, c) 4 wt-% DM, d) 8 wt-% DM; PEG-P(CL30-LLA70) e) 4 wt-% AS f) 8 wt-% AS, g) 4 wt-% DM, h) 8 wt-% DM; PEG-P(CL30-DLLA70) i) 4 wt-% AS, j) 8 wt-% AS, k) 4 wt-% DM, l) 8 wt-% DM; PEG-P(CL15-DLLA85) m) 4 wt-% AS, h) 8 wt-% AS, o) 4 wt-% DM and p) 8 wt-% DM. Length of scale bar is 1mm for samples a) to l) and 1.5mm for samples m) to p).

3.4. Hydrophilicity

Generally, a static water contact angle less than 90° is defined as hydrophilic while greater than 90° as hydrophobic [43]. However, a cutoff angle of 65° is also proposed, which is based on long-range hydrophobic interactions [44]. Wettability of porous materials is difficult, especially when the pores are small and material is hydrophobic, and therefore incorporation of PEG into the copolymer was assumed to increase the hydrophilicity and decrease the contact angle of the polymers. Table 6 lists the contact angles of dry and wet polymer samples. As can be seen in the table, immersing the PEG-containing samples into water decreases the contact angle significantly. Also the contact angle of P(CL30-LLA70) decreases, but the effect is not so notable.

Table 6. Contact angles of dry (d) and wet (w) materials and number of samples (n).

	d (°)	w (°)	difference (°)	n dry	n wet
P(CL30-LLA70)	72.3±4.5	67.7±6.1	4.6	11	14
PEG-P(CL30-LLA70)	72.1±4.1	59.7±6.0	12.4	8	7
PEG-(PCL30-DLLA70)	68.4±4.5	58.7±4.6	9.7	9	8
PEG-P(Cl15-DLLA85)	67.7±2.6	60.2±6.6	7.5	9	8

3.5. Polymer degradation and swelling

The weight of the samples did not change during the first 8 weeks (Figure 5a). After that, the PEG- containing polymers displayed a significant decrease in weight. Mass loss of PEG-P(CL30-LLA70) started after 12 weeks, and in the case of the commercial P(CL30-LLA70) after 14 weeks. Figure 5b presents the swelling behavior of solid polymer samples. PEG-P(CL15-DLLA85) absorbs 5% of water during the first 24 hours and after 9 days already 20%. PEG-P(CL30-DLLA70) also absorbs water, however the rate is slower. Polymers containing D,L-lactide swell significantly faster compared to polymers containing L-lactide. P(CL30-LLA70) swelled less than 2% during 11 weeks, whereas PEG-P(CL30-LLA70) reached 12% swelling.

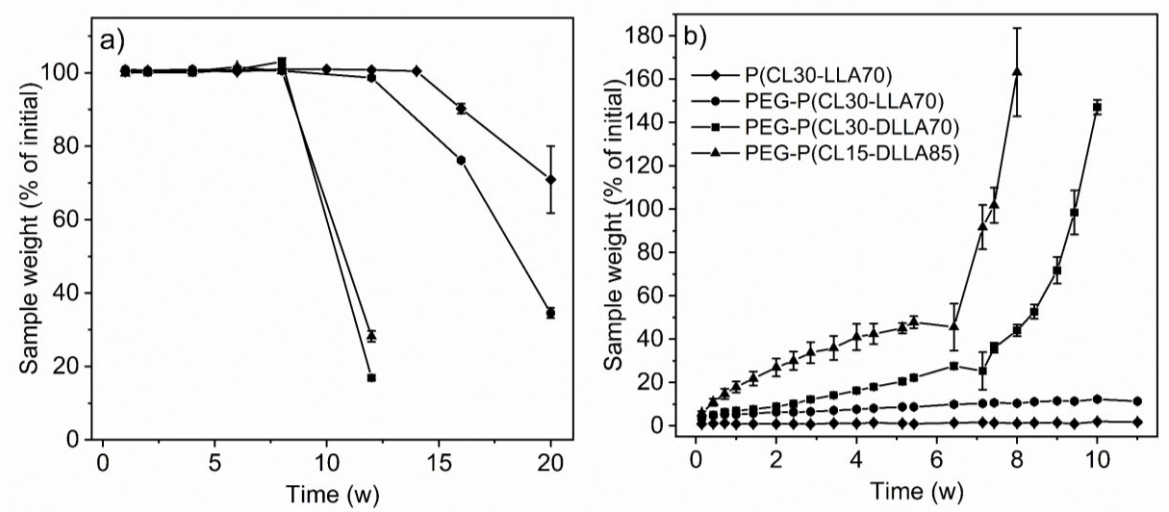

Figure 5. a) Sample weight and b) swelling of solid polymer: P(CL30-LLA70) (♦), PEG-P(CL30-LLA70) (●), PEG-P(CL30-DLLA70) (■) and PEG-P(CL15-DLLA85) (▲).

Figure 6 shows the degradation of solid and porous polymers. Number average molecular weight (M_n) decreased over 50% already after 2 weeks for PEG-containing polymers. Also the M_n of P(CL30-LLA70) decreased relatively fast, 24% in the first two weeks and 36% in 4 weeks. Since there was no change in specimen weight during the first 8 weeks even though the number average molecular weight decreased to at least half compared to the initial M_n, the polymers underwent bulk degradation.

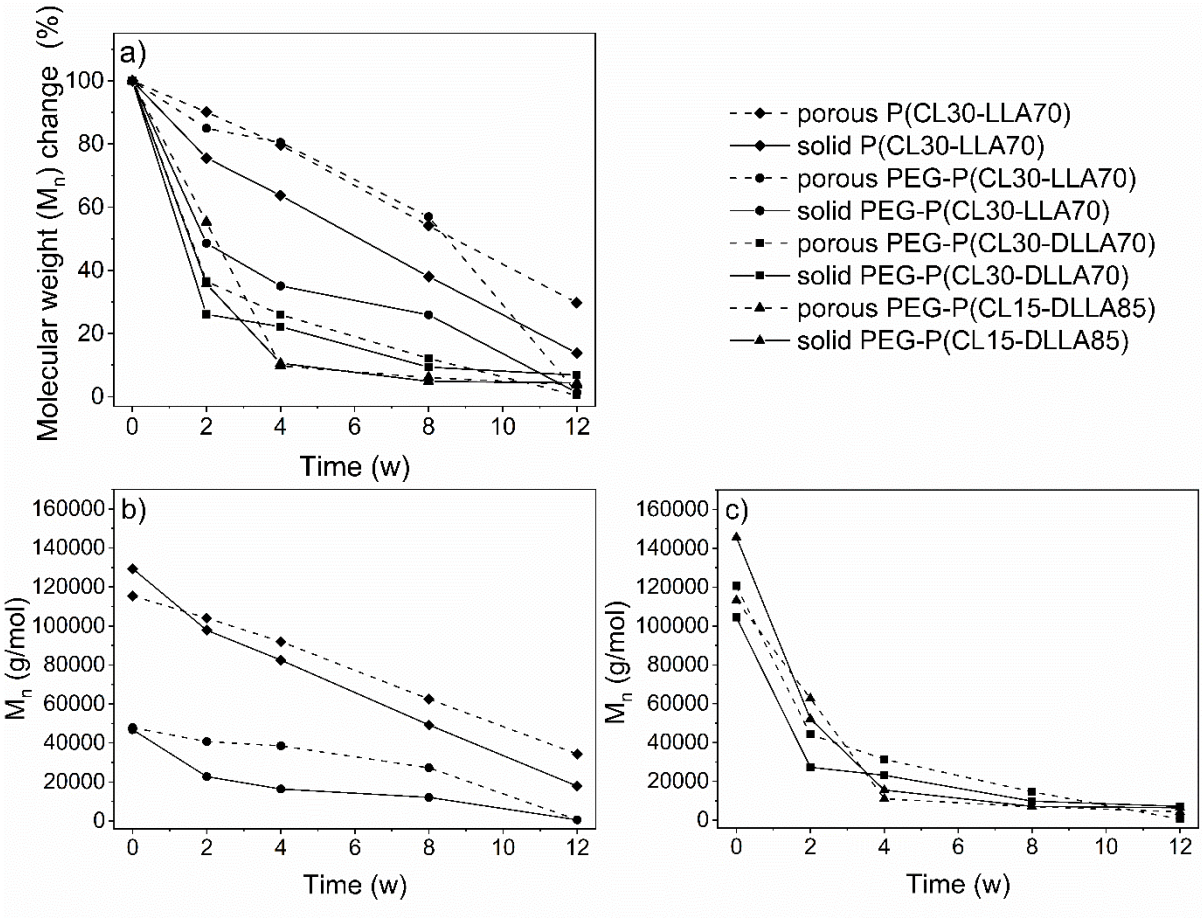

Figure 6. a) Remaining number average molecular weight (% of initial M_n). Molecular weight (M_n) change during hydrolysis for solid and porous samples of b) P(CL30-LLA70) (●) and PEG-P(CL30-LLA70) (♦) and c) PEG-P(CL30-DLLA70) (■) and PEG-P(CL15-DLLA85) (▲).

3.6. Active agent release

Active agent release profiles are shown in Figure 7 for AS and in Figure 8 for DM. In all cases, active agent release is faster from porous samples compared to solid samples. Water-soluble AS (solubility 32g/1000g) releases faster compared to DM having a water solubility of 0.09g/1000g, especially with porous samples, where most of the AS is released within 1 week. According to the active agent stability study, AS was not stable in the experiment conditions. The concentration of AS decreased 4.8% during one week, whereas the concentration of DM did not change.

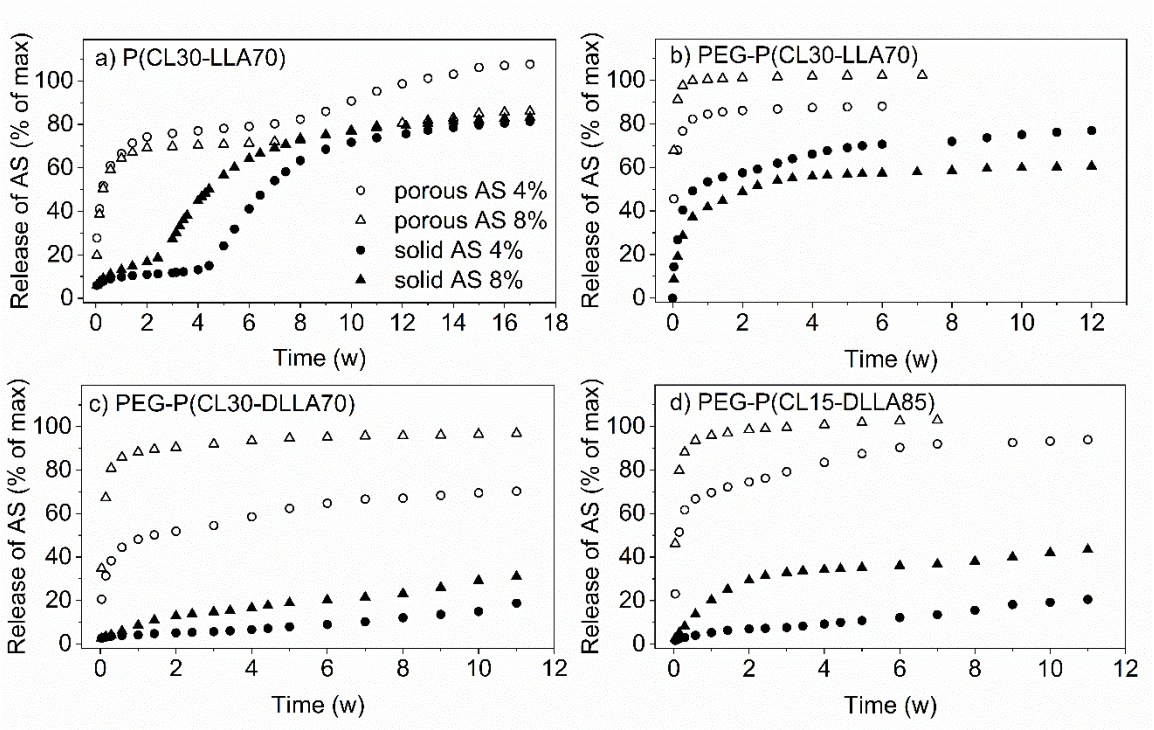

Figure 7. AS release from porous and solid a) P(CL30-LLA70), b) PEG-P(CL30-LLA70), c) PEG-P(CL30-DLLA70) and d) PEG-P(CL15-DLLA85) samples. Difference in time scales is due to different degradation profiles of the polymers.

Solid and porous AS samples exhibited different release profiles (Figure 7). Porous samples release AS with a burst. Compared to the commercial reference, AS release is faster from porous polymers containing PEG probably due to better wettability of the samples. By comparing Figures 7a and 7b, solid PEG-P(CL30-LLA70) releases AS faster than the reference P(CL30-LLA70). This might be due to the faster degradation of PEG-P(CL30-LLA70).

The drug release study was continued for 11 to 12 weeks for PEG-containing samples and 20 weeks for commercial polymer P(CL30-LLA70). Since all solid PEG-containing polymers and especially DL-containing polymers swell in water, AS might degrade inside polymer samples before releasing into the buffer solution; therefore 100 % release was not attained.

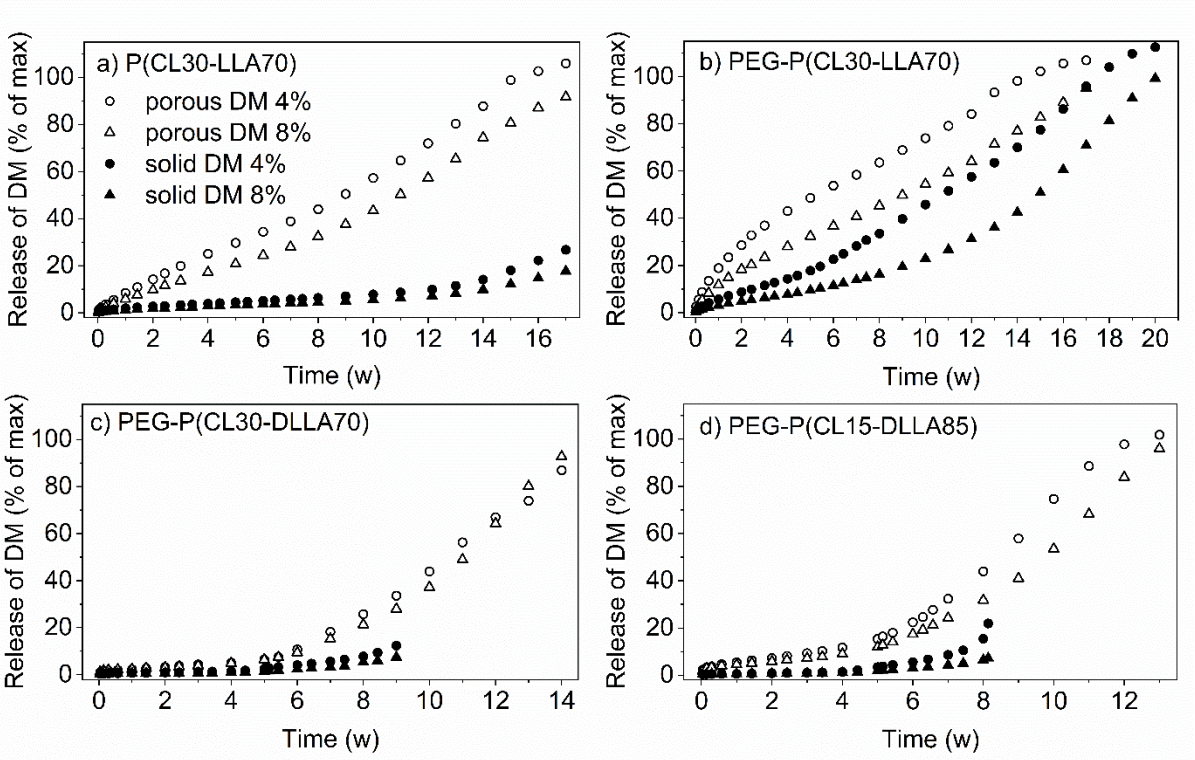

Figure 8. Cumulative DM release (% of max) from porous (p) and solid polymer samples. a) P(CL30-LLA70), b) PEG-P(CL30-LLA70), c) PEG-P(CL30-DLLA70) and d) PEG-P(CL15-DLLA85). There is a different time scale in the graphs due to the different degradation profiles of polymers.

DM release was slower (Figure 8), most probably due to the low water solubility of the molecule, and burst effects seen with porous AS samples were not present. P(CL70-LLA30) and PEG-P(CL30-LLA70) had similar release profiles from porous samples. However, release from solid samples was slower for P(CL30-LLA70), reaching only 27% of the maximum (DM8 samples). Lower release rate from P(CL30-LLA70) is a consequence of the slower degradation of the polymer.

Porous and solid specimens containing D,L-lactide displayed a lag period in the beginning of the dissolution time. The release started to be notable after 5 weeks. After 4 weeks, the molecular mass had decreased already to 9% of the initial molecular mass for PEG-P(CL15-DLLA85) and to 22% for PEG-P(CL30-DLLA70). Therefore, it is suggested that for D,L-lactide containing samples, DM release was initiated also by degradation of the polymer.

4. DISCUSSION

This study presented the strong effect of polymer morphology on the foaming process, since using the same foaming procedure on all polymers, the amorphous polymers (P(CL30-LLA70), PEG-P(CL30-DLLA70) and PEG-P(CL15-DLLA85) had a significantly higher level porosity (range 57-72% as combined) and interconnectivity (>99%) than the semi-crystalline (PEG-P(CL30-LLA70)) (19-31% and 83-95%) respectively, despite the active agent concentration or type. This type of material behavior during processing due to crystallinity has been previously reported with pure polymers [31,45]. The semi-crystalline polymers have been shown to be more difficult to foam compared to amorphous ones [32] and it has been hypothesized that the pores grow specifically on the amorphous regions of the polymer [46]. However, crystalline domains within the polymers may lead to increased pore nucleation rate and pore density during the foaming process and result in a finer pore morphology [47]. The previous research supports findings in this study, as the semi-crystalline polymer reached lower porosity compared to the amorphous ones. If processing is conducted below the melting temperature of crystals, the crystallinity should be low enough to allow effective pore formation [46]. To further improve the porous architecture of semi-crystalline polymer PEG-P(CL30-LLA70), the foaming process could be changed. Modification of processing conditions, especially using processing temperature higher than the melting point of crystals and selecting suitable cooling rate or using co-solvent, have been shown to influence significantly on the porogenization of crystalline polymers [32]. Previously, the porosity of $scCO_2$ foamed biodegradable polymers has been reported to be in the range from 40% to 85%, pore size from 10 to 650µm, and several studies report interconnected porosity [31,32,38,45,48,49]. In many cases the interconnectivity between the pores has, however, been evaluated only with

SEM. The porosity and pore size of foamed polymers prepared in this study are in the same range and the pores were highly interconnected.

Generally with polymer drug blends, the change in a polymer's glass transition temperature can indicate interaction of active agent with the polymer matrix. According to the DSC measurements, DM and AS did not significantly change the glass transition temperatures of polymers, which indicates that the drug particles do not interact with the polymer. In addition, the clear melting peaks of the active agents in the polymer blends supported this observation indicating that both active agents are dispersed in the polymer matrix. However, as the active agent particles could also be detected by micro-CT and the sizes of the particles and average wall thicknesses can be compared easily, it can be noticed that the walls are thin (mean thickness from 48μm up to 99μm) compared to large (diameter over 100μm) AS particles. Therefore, part of the AS particles can be exposed to the buffer solution directly while most of the particles are embedded in the polymer matrix. The DM particles are notably smaller; most of them having a diameter less than 50μm, and thus are likely to be covered with polymer. Therefore, the DM particles are less affected by the buffer solution in the porous polymer structures.

The drug release from $scCO_2$ foamed polymers has been studied previously with PCL and PMMA-PLA [35,36,39]. Previously, water soluble drugs have shown burst release and insoluble drug slower release from $scCO_2$ foamed PCL samples [35,36]. In this study, the burst release of water-soluble active agents was also present as well as more prolonged release of less water-soluble dexamethasone. However, scaffolds having low porosity and small average pore size did not have the slowest release rate as previously presented by Salerno *et al.* [35]. Moreover, amongst porous samples, the pore size and porosity did not seem to have an effect

on release, even though active agent release rate was significantly higher in porous samples compared to solid ones. Therefore, the chemical composition of polymer, which affects the wettability and degradation of the polymer samples, might be a more significant factor in the release than the pore architecture.

Swelling and faster degradation have been shown to result in higher ibuprofen release rate from PMMA-PLA blends [39]. In this study, swelling and faster degrading polymers PEG-P(CL30-DLLA70) and PEG-P(CL15-DLLA85) released AS faster from porous samples compared to P(CL30-LLA70) and PEG-P(CL30-LLA70) which degraded slower and did not swell. The incorporation of PEG into the backbone of the polymer increased the release rate of AS, most probably due to the better wettability of porous samples.

Solid polymer samples did not reach 100% release of AS unlike porous ones. The reason might be that the AS degraded in the aqueous environment and even though it was inside the solid polymer samples, there were some moisture present. In particular, D,L-lactide containing polymers swelled in buffer solution and did not release high amounts of AS. Therefore, according to this study, AS would be more suitable for short drug release periods or used with polymers that do not swell due to its relatively fast degradation in water.

The amounts of DM and ascorbic acid 2-phosphate used in osteogenic differentiation media have been in the range of 10nM (3.92ng/ml) to 100nM (39.2ng/ml) and 10nM (3.2ng/ml) to 0.25mM (80.5mg/ml), respectively [13,50–52]. For porous P(CL30-LLA70) and PEG-P(CL30-LLA70) scaffolds the dexamethasone concentration was between 1-10μg/ml. Porous PEG-P(CL30-DLLA70) and PEG-P(CL15-DLLA85) had slightly lower concentrations during the first 4-5 weeks (0.2-1.4μg/ml) and higher (1.2-25μg/ml) in the end. The concentration of DM is significantly higher compared to amounts used in cell cultures and lower amounts of DM

would most probably be enough. The solubility of DM in water is 90μg/ml. Therefore, the release was not controlled by the solubility of DM. In this study, AS was released by burst from the polymers. Thus, its concentration was higher in the beginning (weeks 1-2) 6-85μg/ml and lower in the end (0.2-2.5μg/ml). Depending on the actual optimal dose of AS, the concentration is in the range of the effective level. It is, however, significantly lower compared to the highest amounts of ascorbic acid 2-phosphate used in osteogenic differentiation media [13,50]. Incorporation of both dexamethasone and ascorbate-2-phosphate in porous PLGA scaffolds has been shown to increase the mesenchymal stem cell osteogenesis *in vitro* [14]. Usually, both of the agents have been used in osteogenic differentiation media [13,51,52]; therefore, it would be beneficial to incorporate both of the agents into the scaffolds.

5. CONCLUSION

Four co-polymers of poly(ethylene glycol), ε-caprolactone, L-lactide and D,L-lactide were blended with two bone regeneration enhancing active agents; 2-phospho-L-ascorbic acid trisodium salt (AS) and dexamethasone (DM). Blends were foamed with $scCO_2$ resulting in amorphous polymers with high interconnectivity and porosity range of 57-72%, and semi-crystalline polymer with lower interconnectivity and porosity, as analyzed by μCT. Concentration or type of the active agent did not affect the porous architecture.

Water-soluble AS released through diffusion with burst, whereas DM released during several weeks by polymer degradation. Porosity accelerated the drug release of AS significantly and DM slightly compared to solid samples. The polymer and drug compositions were the most significant factors in the drug release. The most promising combinations for active agent release are porous DM containing P(CL30-LLA70) and PEG-P(CL30-LLA70). The release with

these combinations is controlled and especially porous samples showed near zero order release kinetics up to 18-20 weeks.

ACKNOWLEDGEMENTS

The authors would like to thank Jenny and Antti Wihuri Foundation and The Finnish Funding Agency for Innovation, Tekes, for providing funding for this project. This work has made use of BIOECONOMY infrastructure at Aalto University.

Declarations of interest: none.

The raw/processed data required to reproduce these findings cannot be shared at this time due to technical or time limitations.

[1] O. Faour, R. Dimitriou, C.A. Cousins, P. V. Giannoudis, The use of bone graft substitutes in large cancellous voids: Any specific needs?, Injury. 42 (2011) S87–S90. doi:10.1016/j.injury.2011.06.020.

[2] V. Campana, G. Milano, E. Pagano, M. Barba, C. Cicione, G. Salonna, W. Lattanzi, G. Logroscino, Bone substitutes in orthopaedic surgery: from basic science to clinical practice, J. Mater. Sci. Mater. Med. 25 (2014) 2445–2461. doi:10.1007/s10856-014-5240-2.

[3] K.U. Lewandrowski, J. D. Gresser, D.L. Wise, D.J. Trantolo, Bioresorbable bone graft substitutes of different osteoconductivities: A histologic evaluation of osteointegration of poly(propylene glycol-co-fumaric acid)-based cement implants in rats, Biomaterials. 21 (2000) 757–764. doi:10.1016/S0142-9612(99)00179-9.

[4] J. Van Der Stok, E.M.M. Van Lieshout, Y. El-Massoudi, G.H. Van Kralingen, P. Patka, Bone substitutes in the Netherlands - A systematic literature review, Acta Biomater. 7 (2011) 739–750. doi:10.1016/j.actbio.2010.07.035.

[5] A.S. Brydone, D. Meek, S. MacLaine, Bone grafting, orthopaedic biomaterials, and the clinical need for bone engineering, Proc. Inst. Mech. Eng. Part H J. Eng. Med. 224 (2010) 1329–1343. doi:10.1243/09544119JEIM770.

[6] L. Pryor, E. Gage, C.-J. Langevin, F. Herrera, A. Breithaupt, C. Gordon, A. Afifi, J. Zins, H. Meltzer, A. Gosman, S. Cohen, R. Holmes, Review of Bone Substitutes, Craniomaxillofacial Trauma Reconstr. 2 (2009) 151–160. doi:10.1055/s-0029-1224777.

[7] D.D. Hile, M.L. Amirpour, A. Akgerman, M. V Pishko, Active growth factor delivery from poly (D , L -lactide-co- glycolide) foams prepared in supercritical CO 2, J. Control. Release. 66 (2000) 177–185.

[8] M.Z. Moghadam, S. Hassanajili, F. Esmaeilzadeh, M. Ayatollahi, M. Ahmadi, Formation of porous HPCL/LPCL/HA scaffolds with supercritical CO2gas foaming method, J. Mech. Behav. Biomed. Mater. 69 (2017) 115–127. doi:10.1016/j.jmbbm.2016.12.014.

[9] S.M. Howdle, M.S. Watson, M.J. Whitaker, V.K. Popov, M.C. Davies, F.S. Mandel, J.D. Wang, K.M. Shakesheff, Supercritical fluid mixing: Preparation of thermally sensitive polymer composites containing bioactive materials, Chem. Commun. (2001) 109–110. doi:10.1039/b008188o.

[10] H.M. Aydin, E. Pişkin, A. Çalimli, Microporous scaffolds from poly(lactide-co-ε-caprolactone) composites with hydroxyapatite and tricalcium phosphates using supercritical CO2 for bone tissue engineering, J. Bioact. Compat. Polym. 19 (2004) 383–

394. doi:10.1177/0883911504046688.

[11] L.M. Mathieu, M.O. Montjovent, P.E. Bourban, D.P. Pioletti, J.A.E. Månson, Bioresorbable composites prepared by supercritical fluid foaming, J. Biomed. Mater. Res. - Part A. 75 (2005) 89–97. doi:10.1002/jbm.a.30385.

[12] L. Elomaa, A. Kokkari, T. Närhi, J. V. Seppälä, Porous 3D modeled scaffolds of bioactive glass and photocrosslinkable poly(ε-caprolactone) by stereolithography, Compos. Sci. Technol. 74 (2013) 99–106. doi:10.1016/j.compscitech.2012.10.014.

[13] A. Wang, X. Ding, S. Sheng, Z. Yao, Bone morphogenetic protein receptor in the osteogenic differentiation of rat bone marrow stromal cells, Yonsei Med. J. 51 (2010) 740–745. doi:10.3349/ymj.2010.51.5.740.

[14] H. Kim, H.W. Kim, H. Suh, Sustained release of ascorbate-2-phosphate and dexamethasone from porous PLGA scaffolds for bone tissue engineering using mesenchymal stem cells, Biomaterials. 24 (2003) 4671–4679. doi:10.1016/S0142-9612(03)00358-2.

[15] T. Yoshikawa, H. Ohgushi, M. Akahane, S. Tamai, K. Ichijima, Analysis of gene expression in osteogenic cultured marrow/hydroxyapatite construct implanted at ectopic sites: A comparison with the osteogenic ability of cancellous bone, J. Biomed. Mater. Res. 41 (1998) 568–573. doi:10.1002/(SICI)1097-4636(19980915)41:4<568::AID-JBM8>3.0.CO;2-A.

[16] H. Kim, H. Suh, S.A. Jo, H.W. Kim, J.M. Lee, E.H. Kim, Y. Reinwald, S.H. Park, B.H. Min, I. Jo, In vivo bone formation by human marrow stromal cells in biodegradable scaffolds that release dexamethasone and ascorbate-2-phosphate, Biochem. Biophys. Res.

Commun. 332 (2005) 1053–1060. doi:10.1016/j.bbrc.2005.05.051.

[17] C. Wu, R. Miron, A. Sculean, S. Kaskel, T. Doert, R. Schulze, Y. Zhang, Proliferation, differentiation and gene expression of osteoblasts in boron-containing associated with dexamethasone deliver from mesoporous bioactive glass scaffolds, Biomaterials. 32 (2011) 7068–7078. doi:10.1016/j.biomaterials.2011.06.009.

[18] R. Gundle, C.J. Joyner, J.T. Triffitt, Human Bone Tissue Formation in-Diffusion Chamber Culture in-Vivo by Bone-Derived Cells and Marrow Stromal Fibroblastic Cells, Bone. 16 (1995) 597–601. doi:Doi 10.1016/8756-3282(95)00112-Q.

[19] J.J. Yoon, J.H. Kim, T.G. Park, Dexamethasone-releasing biodegradable polymer scaffolds fabricated by a gas-foaming/salt-leaching method, Biomaterials. 24 (2003) 2323–2329. doi:10.1016/S0142-9612(03)00024-3.

[20] P. Špiclin, M. Homar, A. Zupančič-Valant, M. Gašperlin, Sodium ascorbyl phosphate in topical microemulsions, Int. J. Pharm. 256 (2003) 65–73. doi:10.1016/S0378-5173(03)00063-2.

[21] R. Austria, A. Semenzato, A. Bettero, Stability of vitamin C derivatives in solution and topical formulations, J. Pharm. Biomed. Anal. 15 (1997) 795–801. doi:10.1016/S0731-7085(96)01904-8.

[22] G. Hannink, J.J.C. Arts, Bioresorbability, porosity and mechanical strength of bone substitutes: What is optimal for bone regeneration?, Injury. 42 (2011) S22–S25. doi:10.1016/j.injury.2011.06.008.

[23] Q.L. Loh, C. Choong, Three-Dimensional Scaffolds for Tissue Engineering Applications: Role of Porosity and Pore Size, Tissue Eng. Part B Rev. 19 (2013) 485–502.

doi:10.1089/ten.teb.2012.0437.

[24] C.M. Murphy, M.G. Haugh, F.J. O'Brien, The effect of mean pore size on cell attachment, proliferation and migration in collagen-glycosaminoglycan scaffolds for bone tissue engineering, Biomaterials. 31 (2010) 461–466. doi:10.1016/j.biomaterials.2009.09.063.

[25] A. Salerno, E. Di Maio, S. Iannace, P.A. Netti, Solid-state supercritical CO2foaming of PCL and PCL-HA nano-composite: Effect of composition, thermal history and foaming process on foam pore structure, J. Supercrit. Fluids. 58 (2011) 158–167. doi:10.1016/j.supflu.2011.05.009.

[26] D.D. Hile, M. V Pishko, Emulsion Copolymerization of D , L -Lactide and Glycolide in Supercritical Carbon Dioxide, (2001) 6–8.

[27] M. Bhamidipati, A.M. Scurto, M.S. Detamore, The Future of Carbon Dioxide for Polymer Processing in Tissue Engineering, Tissue Eng. Part B Rev. 19 (2013) 221–232. doi:10.1089/ten.teb.2012.0361.

[28] D. Rouholamin, P.J. Smith, E. Ghassemieh, Control of morphological properties of porous biodegradable scaffolds processed by supercritical CO2foaming, J. Mater. Sci. 48 (2013) 3254–3263. doi:10.1007/s10853-012-7109-4.

[29] S.K. Goel, E.J. Beckman, Generation of microcellular polymeric foams using supercritical carbon dioxide. II: Cell growth and skin formation, Polym. Eng. Sci. 34 (1994) 1148–1156. doi:10.1002/pen.760341408.

[30] S.P. Nalawade, F. Picchioni, J.H. Marsman, L.P.B.M. Janssen, The FT-IR studies of the interactions of CO2 and polymers having different chain groups, J. Supercrit. Fluids. 36

(2006) 236–244. doi:10.1016/j.supflu.2005.06.005.

[31] D.J. Mooney, D.F. Baldwin, N.P. Suh, J.P. Vacanti, R. Lanrger, Novel approach to fabricate porous sponges of poly (l,d-lactic-co-glycolic acid) without the use of organic solvents, Biomaterials. 17 (1996) 1417–1422.

[32] C. Gualandi, L.J. White, L. Chen, R.A. Gross, K.M. Shakesheff, S.M. Howdle, M. Scandola, Scaffold for tissue engineering fabricated by non-isothermal supercritical carbon dioxide foaming of a highly crystalline polyester, Acta Biomater. 6 (2010) 130–136. doi:10.1016/j.actbio.2009.07.020.

[33] M. Morisaki, T. Ito, M. Hayvali, I. Tabata, K. Hisada, T. Hori, Preparation of skinless polymer foam with supercritical carbon dioxide and its application to a photoinduced hydrogen evolution system, Polymer (Guildf). 49 (2008) 1611–1619. doi:10.1016/j.polymer.2008.01.049.

[34] H. Pihlman, P. Keränen, K. Paakinaho, J. Linden, M. Hannula, I.-K. Manninen, J. Hyttinen, M. Manninen, O. Laitinen-Vapaavuori, Novel osteoconductive β-tricalcium phosphate/poly(L-lactide-co-e-caprolactone) scaffold for bone regeneration: a study in a rabbit calvarial defect, J. Mater. Sci. Mater. Med. 29 (2018) 156. doi:10.1007/s10856-018-6159-9.

[35] A. Salerno, J. Saurina, C. Domingo, Supercritical CO2foamed polycaprolactone scaffolds for controlled delivery of 5-fluorouracil, nicotinamide and triflusal, Int. J. Pharm. 496 (2015) 197–204. doi:10.1016/j.ijpharm.2015.11.012.

[36] R. Yoganathan, R. Mammucari, N.R. Foster, Impregnation of Ibuprofen into Polycaprolactone using supercritical carbon dioxide, J. Phys. Conf. Ser. 215 (2010).

doi:10.1088/1742-6596/215/1/012087.

[37] J.M. Kanczler, P.J. Ginty, J.J.A. Barry, N.M.P. Clarke, S.M. Howdle, K.M. Shakesheff, R.O.C. Oreffo, The effect of mesenchymal populations and vascular endothelial growth factor delivered from biodegradable polymer scaffolds on bone formation, Biomaterials. 29 (2008) 1892–1900. doi:10.1016/j.biomaterials.2007.12.031.

[38] J.M. Kanczler, P.J. Ginty, L. White, N.M.P. Clarke, S.M. Howdle, K.M. Shakesheff, R.O.C. Oreffo, The effect of the delivery of vascular endothelial growth factor and bone morphogenic protein-2 to osteoprogenitor cell populations on bone formation, Biomaterials. 31 (2010) 1242–1250. doi:10.1016/j.biomaterials.2009.10.059.

[39] D. Velasco, L. Benito, M. Fernández-Gutiérrez, J. San Román, C. Elvira, Preparation in supercritical CO2of porous poly(methyl methacrylate)-poly(l-lactic acid) (PMMA-PLA) scaffolds incorporating ibuprofen, J. Supercrit. Fluids. 54 (2010) 335–341. doi:10.1016/j.supflu.2010.05.012.

[40] T. Seppala, J Hiljanen-Vainio, M Karjalainen, Biodegradable Lactone Copolymers. I. Characterization and Mechanical Behavior of epsilon-Caprolactone and Lactide Copolymers, J. Appl. Polym. Sci. 59 (1996) 1281–1288. doi:10.1002/(SICI)1097-4628(19960222)59:8<1281::AID-APP11>3.0.CO;2-9.

[41] J. Schindelin, I. Arganda-Carreras, E. Frise, V. Kaynig, M. Longair, T. Pietzsch, S. Preibisch, C. Rueden, S. Saalfeld, B. Schmid, J.-Y. Tinevez, D.J. White, V. Hartenstein, K. Eliceiri, P. Tomancak, A. Cardona, Fiji: an open-source platform for biological-image analysis, Nat. Methods. 9 (2012) 676. http://dx.doi.org/10.1038/nmeth.2019.

[42] M. Doube, M.M. Klosowski, I. Arganda-Carreras, F.P. Cordelières, R.P. Dougherty, J.S.

Jackson, B. Schmid, J.R. Hutchinson, S.J. Shefelbine, BoneJ: Free and extensible bone image analysis in ImageJ, Bone. 47 (2010) 1076–1079. doi:10.1016/j.bone.2010.08.023.

[43] K.-Y. Law, Definitions for Hydrophilicity, Hydrophobicity, and Superhydrophobicity: Getting the Basics Right, J. Phys. Chem. Lett. 5 (2014) 686–688. doi:10.1021/jz402762h.

[44] E.A. Vogler, Structure and reactivity of water at bioimaterial surfaces, Adv. Colloid Interface Sci. 74 (1998) 69–117.

[45] J.J.A. Barry, M.M.C.G. Silva, S.H. Cartmell, R.E. Guldberg, C.A. Scotchford, S.M. Howdle, Porous methacrylate tissue engineering scaffolds: Using carbon dioxide to control porosity and interconnectivity, J. Mater. Sci. 41 (2006) 4197–4204. doi:10.1007/s10853-006-7023-8.

[46] S. Doroudiani, C.B. Park, M.T. Kortschot, Doroudiani, Park, Kortschot - 1996 - Effect of the crystallinity and morphology on the microcellular foam structure of semicrystalline polymers.pdf, Polym. Eng. Sci. 36 (1996) 2645–2662.

[47] T. Kuang, F. Chen, L. Chang, Y. Zhao, D. Fu, X. Gong, X. Peng, Facile preparation of open-cellular porous poly (L-lactic acid) scaffold by supercritical carbon dioxide foaming for potential tissue engineering applications, Chem. Eng. J. 307 (2017) 1017–1025. doi:10.1016/j.cej.2016.09.023.

[48] M.J. Jenkins, K.L. Harrison, M.M.C.G. Silva, M.J. Whitaker, K.M. Shakesheff, S.M. Howdle, Characterisation of microcellular foams produced from semi-crystalline PCL using supercritical carbon dioxide, Eur. Polym. J. 42 (2006) 3145–3151. doi:10.1016/j.eurpolymj.2006.07.022.

[49] C. Ji, N. Annabi, M. Hosseinkhani, S. Sivaloganathan, F. Dehghani, Fabrication of poly-DL-lactide/polyethylene glycol scaffolds using the gas foaming technique, Acta Biomater. 8 (2012) 570–578. doi:10.1016/j.actbio.2011.09.028.

[50] S. Takamizawa, Y. Maehata, K. Imai, H. Senoo, S. Sato, R.I. Hata, Effects of ascorbic acid and ascorbic acid 2-phosphate, a long-acting vitamin C derivative, on the proliferation and differentiation of human osteoblast-like cells, Cell Biol. Int. 28 (2004) 255–265. doi:10.1016/j.cellbi.2004.01.010.

[51] N. Eelam Jaiswal, S.E.H. Aynesworth, A.I. Caplan, S.P. Bruder, Osteogenic Differentiation of Purified, Culture-Expanded Human Mesenchymal Stem Cells In Vitro, J. Cell. Biochem. 64 (1997) 295–312.

[52] S.. Park, R.O.. Oreffo, J.. Triffitt, Interconversion potential of cloned human marrow adipocytes in vitro, Bone. 24 (1999) 549–554. doi:10.1016/S8756-3282(99)00084-8.